

## Local Structure Quantification in Tetragonal Tungsten Bronze Structures Utilizing Convolutional Neural Networks

Nicole Creange<sup>1</sup>, Mathew Cabral<sup>2</sup>, Stephen Funni<sup>1</sup>, Zijin Yang<sup>3</sup>, Xiaoli Zhu<sup>3</sup>, Xiangming Chen<sup>3</sup> and Elizabeth Dickey<sup>1</sup>

<sup>1</sup>North Carolina State University, Raleigh, North Carolina, United States, <sup>2</sup>University of Sydney, Sydney, New South Wales, Australia, <sup>3</sup>Zhejiang University, Hangzhou, Zhejiang, China (People's Republic)

The complex structures of relaxor ferroelectrics have been highly studied for over four decades due to their effectiveness for energy storage and energy conversion [1-4]. While perovskite materials are typically used to study ferroelectrics, the perovskite derivative, tetragonal tungsten bronze (TTB) compounds, constitute the second largest family of ferroelectrics [4]. This structure, shown in Figure 1, is comprised of ten corner-shared oxygen octahedra, which form three kinds of cation interstitial sites: A1 square sites, A2 pentagonal sites, and C trigonal sites. The TTB structure can accommodate a wide variety of compositions due to its large structural manipulation ability [4]. With this range of compositions, the properties can also range from classical to relaxor ferroelectric behavior by changing the cation compositions and by partially or fully filling the A1, A2, and C sites. Even with the broad range of dielectric properties, all compositions with the TTB structure exhibit structural modulations believed to arise due to the tilting of the oxygen octahedra. There are two types of structural modulations that can be observed as satellite spots in the diffraction pattern, commensurate with wave vector  $\mathbf{q} = \frac{1}{2}(\mathbf{a}^* + \mathbf{b}^* + \mathbf{c}^*)$  and incommensurate with wave vector  $\mathbf{q} = (\frac{1}{4} + \delta)(\mathbf{a}^* + \mathbf{b}^*) + \frac{1}{2}\mathbf{c}^*$  [5,6]. The incommensurate modulation tends to be associated with relaxor behavior and the transition from commensurate to incommensurate modulation tends to coincide with the ferroelectric to relaxor transition [5,6]. While these structural modulations have been observed in reciprocal space, there is still a lack of detailed real-space structural studies, which could provide more insight into sublattice-specific structural modulations. Recent advancements in aberration-corrected scanning transmission electron microscopy (STEM) and data analysis are providing new insight into the local structure of these materials. Quantification of the local cation disorder could illuminate correlations between the relaxor/ferroelectric behavior and incommensurate/commensurate modulations. However, with a more complex structure than the typical perovskite, the identification and classification of atom columns in STEM images becomes more difficult. Here, in order to locate atom column positions, a convolutional neural network (CNN) is used through the open python package AICrystallographer [7]. Training data sets are created using simulated high angle angular dark field images along the [001]/[110] zone axis with varied magnifications and image rotation. Correspondingly, the resulting training weights are used to determine the (x,y) coordinates of each atom column. Once the atom column positions are identified, the classification of each column is performed via local neighborhood analysis. For this classification, first the distance between each atom column is calculated, then based on the number of nearest neighbors around an atom column, the site is classified as either A1, A2, B1 or B2. A cross-reference to the type of nearest neighbor is performed during the classification to ensure the correct classification of the atom column. From this analysis, we quantify atomic-column intensities, distortions, and positions with picometer-scale precision. Local sublattice distances between each nearest-neighbor similar sublattice site (A1-A1, A2-A2, B1-B1, B2-B2) are presented in Figure 3. Individual distances are shown in Figure 3 a-d while the average distance per atom column can be seen in Figure 3 e-h. Looking at the average distances for the A1 and B2 sublattices shown in Figure 3 e,h we see that there are local regions with an lower average distance and some with a higher average distance with a spread of 0.4 Å. In comparison, the A2 and B2 sublattices do not exhibit any local

clustering of the distances. In addition, the periodicity of the distance modulation in A1 and B2 are on the order of the incommensurate modulation,  $\mathbf{q}=(\frac{1}{4}+\delta)(\mathbf{a}^*+\mathbf{b}^*)$  or  $\mathbf{q}=(4+\delta)(\mathbf{a}+\mathbf{b})$ . The higher symmetry of these sublattices seems to be more susceptible to the oxygen octahedral tilting than the lower symmetry A2 and B1 sublattices. This work is funded partially through the NSF Grant No. DGE-1633587.

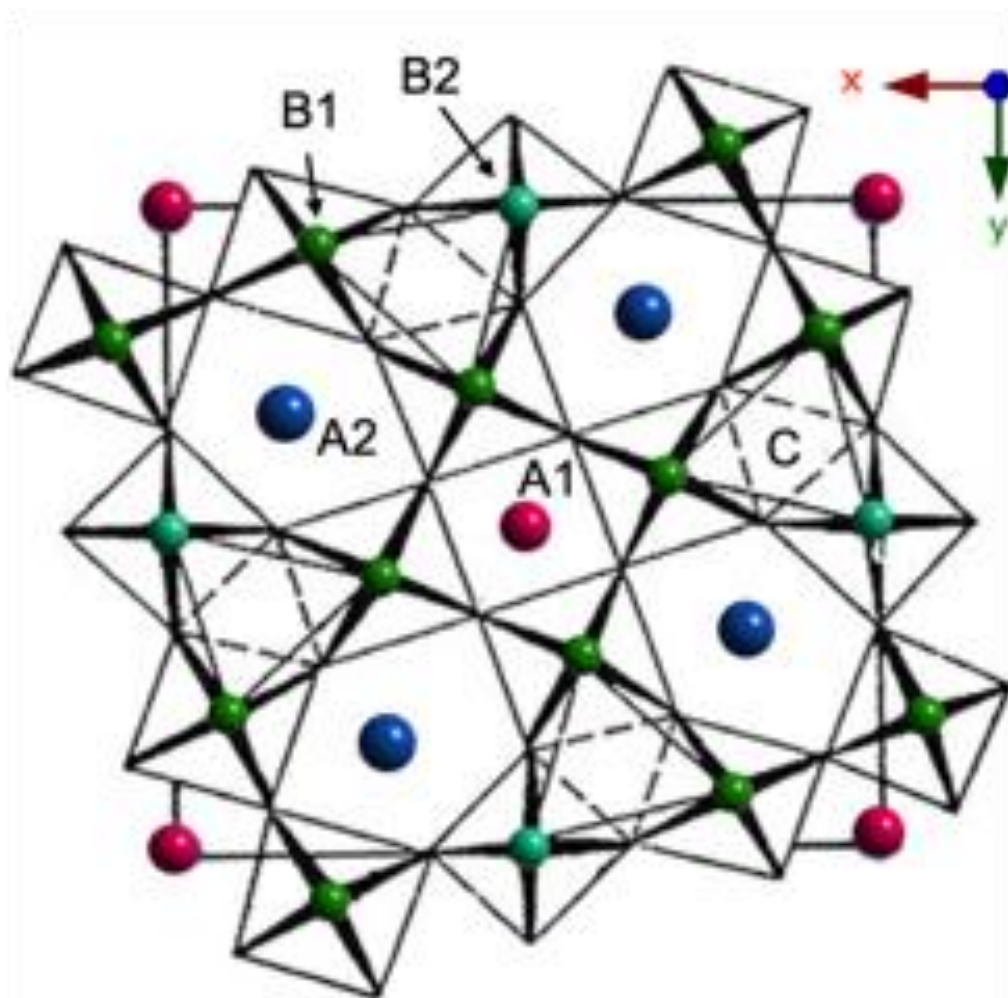


**Figure 1.** [001] projection of the tetragonal tungsten bronze structure showing filled A1, A2 sites and empty C sites.

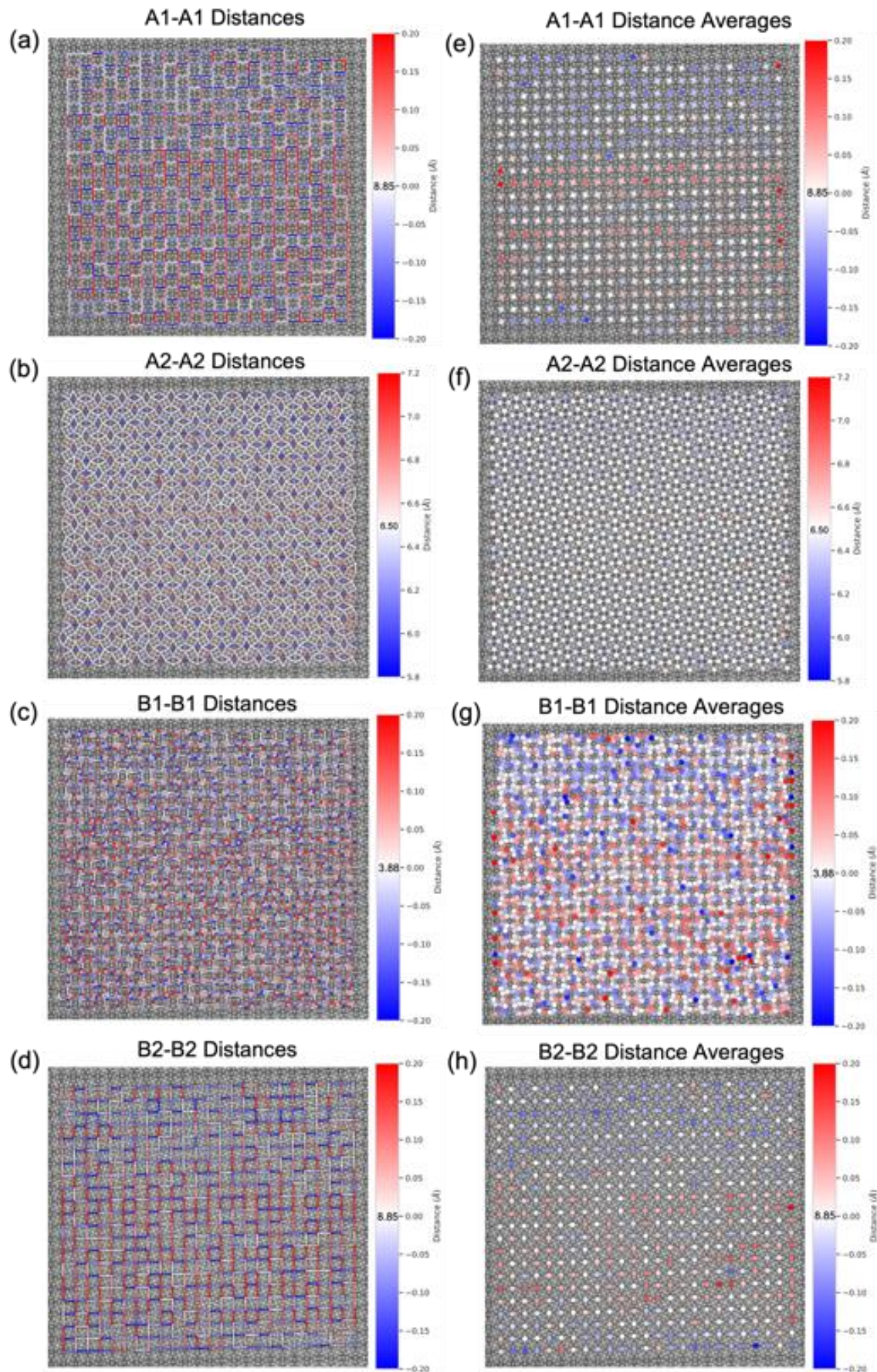


**Figure 2.** Sublattice distance (a-d) and the average distance per site on each sublattice (e-h).

#### References

1. Shrout TR, Zhang SJ. (2007), “Lead-free piezoelectric ceramics: alternatives for PZT?,” *J Electroceram*, 19(1), 113–26.
2. Mischenko AS, Zhang Q, Whatmore RW, Scott JF, Mathur ND. (2006), “Giant electrocaloric effect in the thin film relaxor ferroelectric 0.9 PbMg $_{1/3}$ Nb $_{2/3}$ O $_3$ -1 PbTiO $_3$  near room temperature,” *Appl Phys Lett*. 89(24), 242912.
3. Tong S, Ma BH, Narayanan M, Liu SS, Koritala R, Balachandran U, et al. (2013), “Lead lanthanum zirconate titanate ceramic thin films for energy storage,” *ACS Appl Mater Interfaces*. 5(4), 1474–80.
4. Yang, Z. J., Feng, W. Bin, Liu, X. Q., Zhu, X. L., & Chen, X. M. (2019). “Ba $_4$ R $_2$ Sn $_4$ Nb $_6$ O $_30$  (R = La, Nd, Sm) lead-free relaxors with filled tungsten bronze structure,” *Am. Ceram. Soc.*, 102(8), 4721–4729.
5. Levin, I., Stennett, M. C., Miles, G. C., Woodward, D. I., West, A. R., & Reaney, I. M. (2006), “Coupling between octahedral tilting and ferroelectric order in tetragonal tungsten bronze-structured dielectrics,” *App Phys Lett*. 89(12), 122908.
6. Zhu, X., Fu, M., Stennett, M. C., Vilarinho, P. M., Levin, I., Randall, C. A., ... Reaney, I. M. (2015), “A Crystal-chemical framework for relaxor versus normal ferroelectric behavior in tetragonal tungsten bronzes,” *Mater.*, 27(9), 3250–3261.
7. Ziatdinov, M., Dyck, O., Maksov, A., Li, X., Sang, X., Xiao, K., ... Kalinin, S. V. (2017), “Deep Learning of Atomically Resolved Scanning Transmission Electron Microscopy Images: Chemical Identification and Tracking Local Transformations,” *ACS Nano*, 11(12), 12742–12752